Journal of Molecular Structure xxx (2016) 1–11

Contents lists available at ScienceDirect

Journal of Molecular Structure

journal homepage: http://www.elsevier.com/locate/molstruc

Synthesis of novel anthraquinones: Molecular structure, molecular chemical reactivity descriptors and interactions with DNA as antibiotic and anti-cancer drugs

Jamelah S. Al-Otaibi [a, b], Tarek M. EL Gogary [c, *]

[a] Department of Chemistry, College of Science, Princess Nourah bint Abdulrahman University, Riyadh 11951, Saudi Arabia
[b] Deanship of Scientific Research, Princess Nora Bint Abdul Rahman University, Saudi Arabia
[c] Department of Chemistry, Faculty of Science, Jazan University, Jazan, Saudi Arabia

ARTICLE INFO

Article history:
Received 29 August 2016
Received in revised form
30 October 2016
Accepted 31 October 2016
Available online xxx

Keywords:
Anthraquinone
Anti-cancer
Reactivity descriptors
NMR
Scatchard analysis

ABSTRACT

Anthraquinones are well-known anticancer drugs. Anthraquinones anticancer drugs carry out their cytotoxic activities through their interaction with DNA, and inhibition of topoisomerase II activity. Anthraquinones (AQ5 and AQ5H) were synthesized and studied with 1,5-DAAQ by computational and experimental tools. The purpose of this study is to shade more light on mechanism of interaction between anthraquinone DNA affinic agents and different types of DNA. This study will lead to gain of information useful for drug design and development. Molecular structures were optimized using DFT B3LYP/6-31 + G(d). Depending on intramolecular hydrogen bonding interactions four conformers of AQ5 were detected within the range of about 42 kcal/mol. Molecular reactivity of the anthraquinone compounds was explored using global and condensed descriptors (electrophilicity and Fukui functions). NMR and UV–VIS electronic absorption spectra of anthraquinones/DNA were investigated at the physiological pH. The interaction of the anthraquinones (AQ5 and AQ5H) were studied with different DNA namely, calf thymus DNA, (Poly[dA].Poly[dT]) and (Poly[dG].Poly[dC]). UV–VIS electronic absorption spectral data were employed to measure the affinity constants of drug/DNA binding using Scatchard analysis. NMR study confirms qualitatively the drug/DNA interaction in terms of peak shift and broadening.

1. Introduction

Quinone-containing compounds are a series of widespread compounds found in nature. Quinones and quinone-derivatives are important class of molecules, having high importance in dye industry, biology and pharmaceutical chemistry [1–7].These compounds are known to perform many biochemical and physiological processes in living organisms. Anthraquinones, as a group of natural quinones, are widely used in treatment of cancer [8–11]. Anthraquinones anticancer drugs carry out their cytotoxic activities through their interaction with DNA, preferentially at guanine/cytocine rich sites [12]. This interaction is believed to cause significant conformational changes in the DNA leading to inhibition of the DNA replication [12]. This may lead to DNA damage. On the other hand, they can cause inhibition of topoisomerase II activity, leading to DNA damage. The development of novel potent chemotherapeutics and design of small drug molecules that selectively target DNA, with high binding constants, has led to the discovery of many anticancer, antibiotic, and antiviral drugs [13–21]. Most DNA-targeted molecules start their binding with double helix DNA non-covalently which subsequently may developed to covalent binding. Non-covalent binding may include π-stacking, hydrogen bonding, electrostatic, charge transfer, and hydrophobic interactions [12]. All these interactions may contribute to the drug/DNA interaction mechanism so that the main objective of this study is to explore the dominant interaction. This information is crucial for design and development of new anthraquinone antibiotic and anticancer drugs.

Of the anthraquinones, the ones having hydroxy and amino substituents have been extensively investigated, to understand their biochemical activity [22–34]. For this study the following amino and hydroxy anthraquinone derivatives (Scheme 1), 1,5-bis {[2-(methylamino)ethyl]amino}-4,8-dihydroxy anthracene-9,10-

* Corresponding author. Department of Chemistry, Faculty of Science, Damietta University, New Damietta City, Egypt.
E-mail address: tarekelgogary@yahoo.com (T.M. EL Gogary).

http://dx.doi.org/10.1016/j.molstruc.2016.10.098
0022-2860/

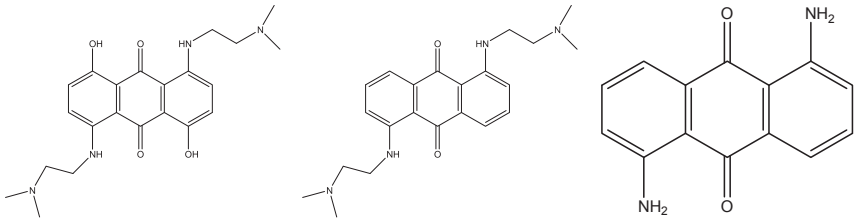

Scheme 1. Studied anthraquinones.

dione, (AQ5), and 1,5-bis{[2-(methylamino)ethyl]amino}anthracene-9,10-dione, (AQ5H) and 1,5-diaminoanthraquinone were chosen for this study.

2. Experimental details

The UV–VIS absorption spectra were measured using a Perkin Elmer Lambda-16 UV–VIS Spectrophotometer. NMR spectra were recorded in $CDCl_3$ using a Bruker AC250 at 30 °C utilizing these experimental parameters: 250 MHz, 5.9 T, 5 mm multinuclear broadband probe, Receiver Gain RG = 8, Pulse Width PW = 4, Relaxation Delay RD = 2 and Number of Scan NS = 8. DNA concentrations per nucleotide were determined spectrophotometrically using the molar absorption coefficient: $\varepsilon_{260} = 6600\ M^{-1}\ cm^{-1}$ to be 1.061×10^{-4} M. NMR spectra of drug/DNA mixtures were measured at 30 °C. Two or three mixture solutions were produced by accurate dilution from the stock solutions keeping AQs concentration constant while varying the concentration of the DNA, were run and compared with the spectra of pure drug. The chemical shift of the AQs bands were measured with reference to the TMS band as internal standard.

Calf thymus DNA, polydeoxyadenylic acid-polythymidylic acid (Poly[dA].Poly[dT]) and polydeoxyguanylic acid-polydeoxycytidylic acid (Poly[dG].Poly[dC]) were purchased from Sigma Chemical Co and were used without further purification. 1,4-DAAQ and D_2O (99.9% D) were purchased from Aldrich. Trizma base (Tris[hydroxymethyl] aminomethane) and NaCl were supplied from Sigma and used for buffer preparation without further purification.

Synthesis of anthraquinone drugs

1,5-bis {[2-(methylamino)ethyl]amino}-4,8-dihydroxy anthracene-9,10-dione, (AQ5), and 1,5-bis{[2-(methylamino)ethyl]amino} anthracene-9,10-dione, (AQ5H) were synthesized according to the following method [35–37]:

AQ5H synthesis

1 1,5-dichloroanthraquinone (15 g, 54 mmol) was dissolved in *N*,*N*-dimethylethylenediamine (47.6 g, 540 mmol) and refluxed for 18 h. The reaction was monitored by TLC (9:1 CH_2Cl_2/MeOH). The mixture was cooled to room temperature and diluted with water to precipitate the title compound. The filtered solid was recrystallized from methanol to afford AQ5H (15.8 g, 89%) as a crystalline solid. R_f(9:1 CH_2Cl_2/MeOH): 0.60. ^{1}H NMR δ ($CDCl_3$): 9.8 (t, 2H), 7.6 (m, 4H), 6.9 (m, 2H), 3.4 (q, 4H), 2.7 (t, 4H), 2.4 (s, 12H). Mass spectrum, *m*/*z* 381 ($m^+ + 1$).

AQ5 synthesis

2 The AQ5H (6 g, 15.8 mmol) was dissolved in 65 g of concentrated sulphuric acid and cooled to −10 °C. Anhydrous sodium chlorate (6.5 g, 61.6 mmol) was added in portions over 1.5 h and the mixture then stirred for 3 h at room temperature. The blue solution was added slowly to cold sodium hydrogen sulfite solution (1%, 1000 cm^3). The mixture was neutralised to pH 7 with 5 M sodium hydroxide. The titled compound was extracted from the aqueous phase with CH_2Cl_2 and concentrated. Column chromatography (SiO_2, (9:1 CH_2Cl_2/MeOH) gave AQ5 (1.2 g, 20%). R_f(9:1 CH_2Cl_2/MeOH):0.17. ^{1}H NMR δ ($CDCl_3$): 13.99 (s, 2H), 9.8 (t, 2H), 7.2 (d, 2H), 7.0 (d, 2H), 3.42 (q, 4H), 2.65 (t, 4H), 2.33 (s, 12H). ^{13}C NMR δ ($CDCl_3$): 186.5, 154.9, 137, 135, 115, 114, 58.1, 45.5, 40.95. Mass spectrum, *m*/*z* 413 ($m^+ + 1$). Anal. Calcd. For $C_{22}H_{28}O_4N_4.0.5H_2O$: C, 62.7; H, 6.7; N, 13.3. Found: C, 62.7; H, 6.9; N, 13.3. UV–VIS Lambda max 642, 600, 238.

3. Computations

All computations were done using G09 suit of programs [38]. Molecular geometry of anthraquinone compounds were optimized in the gas phase at DFT B3LYP/6-31 + G(d,p) level of theory. A frequency job was performed on the optimized geometry to confirm a minimum energy structure. Fukui functions were calculated using DMol^3 module [39,40] employing B3LYP/DND method implemented in Material studio program [41].

4. Results and discussion

4.1. Computational work

4.1.1. Molecular geometry

Since there is no reported experimental molecular geometrical data for AQ5 and AQ5H, we calculated the geometry of AQ5, AQ5H and 1,5-DAAQ at B3LYP/6-31 + G(d). Based on possibility of intra molecular hydrogen bonding formation, four minimum energy conformers, Conf-1, Conf-2, Conf-3 and Conf-4, of AQ5 were studied and displayed in Fig. 1. Conf-1 allows four intra-molecular hydrogen bonds while Conf-2 allows three intra-molecular hydrogen bonds and Conf-3 and Conf-4 allow two and one intra molecular hydrogen bonds respectively (see Fig. 1). The relative total energies differences are shown in Fig. 1. Conf-1 with four intra molecular hydrogen bonds is the most stable structure separating from Conf-4, with only one hydrogen bond, by 41.858 kcal/mol. Conf-2 with three hydrogen bonds is the next stable structure with energy difference 15.762 kcal/mol and Conf-3, with two hydrogen bonds, is separating from Conf-1 by 27.045 kcal/mol. Conformer with no intra molecular hydrogen bonds was also studied however, an optimized minimum structure has not been obtained.

Optimized geometry of AQ5 conformers are shown in Fig. 1. All optimized geometrical parameters of AQ5, Conf-1-4, are represented in Tables S1–S4 in the Supplementary Material. Vibrational frequencies for AQ5 Conf-1 were computed to confirm the minimum energy structure and given in Table S5 in Supplementary Materials.

In Conf-1, the carbonyls bond lengths C_7=O_{15} and $C_{10} = O_{16}$ are identical and calculated as 1.273 Å. The reason for being the same

Please cite this article in press as: J.S. Al-Otaibi, T.M. EL Gogary, Synthesis of novel anthraquinones: Molecular structure, molecular chemical reactivity descriptors and interactions with DNA as antibiotic and anti-cancer drugs, Journal of Molecular Structure (2016), http://dx.doi.org/10.1016/j.molstruc.2016.10.098

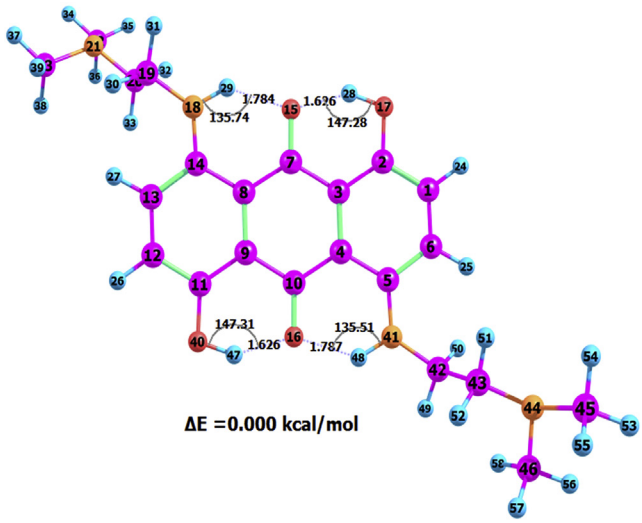

AQ5, Conf-1

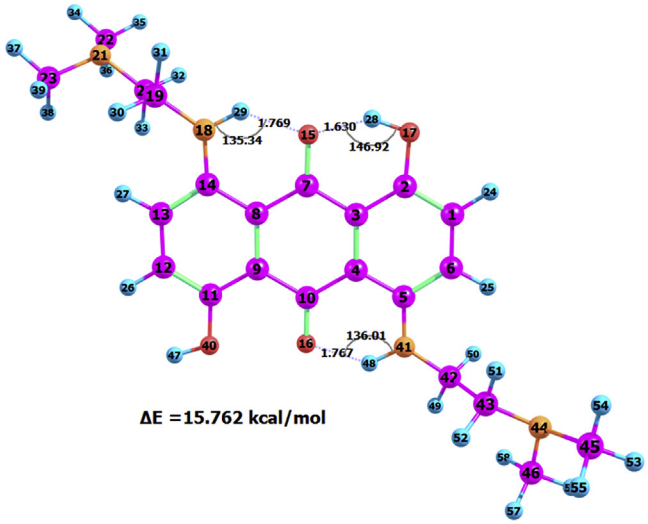

AQ5, Conf-2

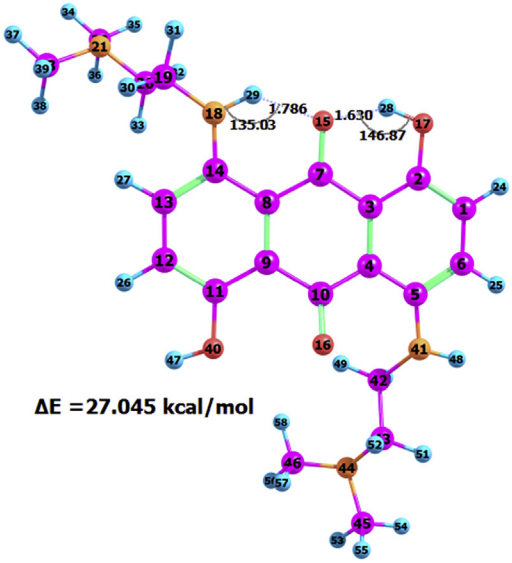

AQ5, Conf-3

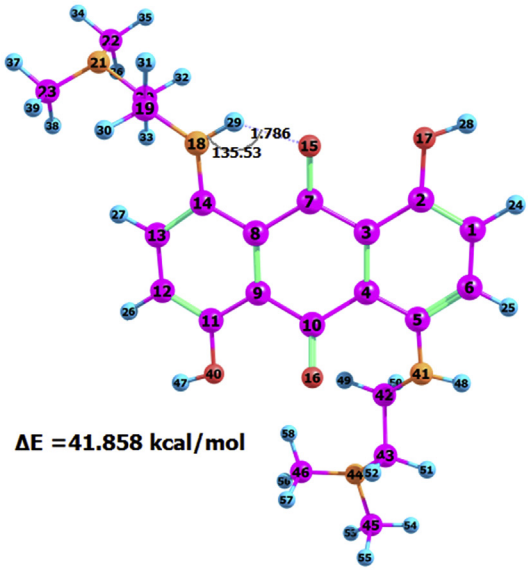

AQ5, Conf-4

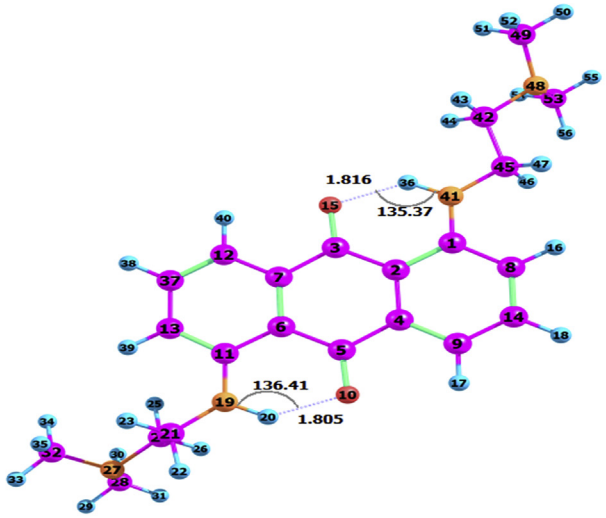

AQ5H

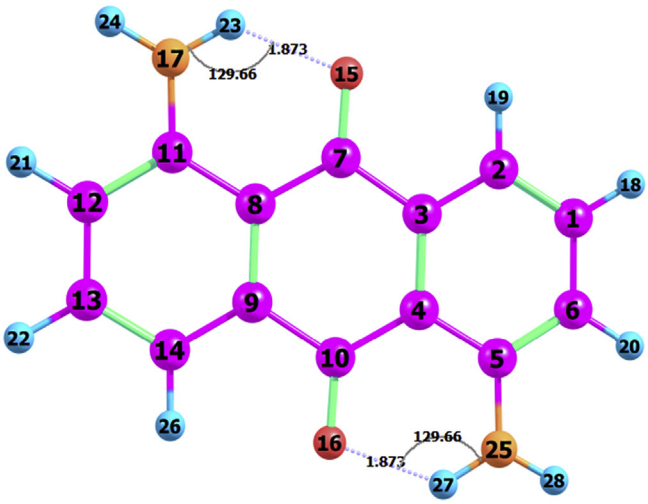

1,5-DAAQ

Fig. 1. Optimized Structure of AQ5 Conf-1-5, AQ5H and 1,5-DAAQ showing atomic numeration and H-bonding.

Please cite this article in press as: J.S. Al-Otaibi, T.M. EL Gogary, Synthesis of novel anthraquinones: Molecular structure, molecular chemical reactivity descriptors and interactions with DNA as antibiotic and anti-cancer drugs, Journal of Molecular Structure (2016), http://dx.doi.org/10.1016/j.molstruc.2016.10.098

length is because of the symmetry of the molecule and the engagement of the O_{15} and O_{16} with two intramolecular hydrogen bonds. Formation of hydrogen bond results in more polarization of the carbonyl group and hence decreasing duple bond character which affect the elongation of the bond. Bond lengths of the two hydrogen bonds, $O_{17}H_{28}\cdots O_{15}$ and $N_{18}H_{29}\cdots O15$ are 1.626 and 1.784 Å respectively. The former hydrogen bond is stronger than the latter. This could be attributed to the higher electronegativity of the O atom with respect to N atom. The angle $C_5{-}C_4{-}C_{10}$ is computed to 121.2° while the corresponding angle $C_2{-}C_3{-}C_7$ is calculated is computed 118.9°. The later angle is decreased to permit effective hydrogen bond interaction. The same argument is true for the angle $C_7{-}C_8{-}C_{14}$ (121.2°) and the angle $C_{10}{-}C_9{-}C_{11}$ (118.9°) where the contraction of the later angle facilitates the $O{-}H\cdots O$ hydrogen bond formation. The ring system in Conf-1 is fully planar as appeared from the values of the dihedral angles, $C_7{-}C_8{-}C_9{-}C_{10}$, $C_{11}{-}C_9{-}C_8{-}C_{14}$, $C_2{-}C_3{-}C_4{-}C_5$, $C_3{-}C_4{-}C_{10}{-}O_{16}$ and $C8{-}C_9{-}C_{10}{-}C_{16}$ which are almost 0.0 and 180.0° (see Table S1).

In AQ5H (Table S6 in Supplementary Materials), the hydrogen bond $N_{19}{-}H_{20}\cdots O_{10}$ is 1.805 Å with an angle $N_{19}{-}H_{20}{-}O_{10}$ 136.4 and hydrogen bond $N_{41}{-}H_{36}\cdots O_{15}$ is 1.816 Å with an angle $N_{41}{-}H_3{-}O_{15}$ 135.4° as shown from Fig. 1. In 1,5-DAAQ, the amino group is planar as shown from Fig. 1. The intra molecular hydrogen bonds $N_{17}{-}H_{23}\cdots O_{15}$ and $N_{25}{-}H_{27}\cdots O_{16}$ are 1.873 Å with a hydrogen bond angle 129.7° as shown from Fig. 1. This similarity of the hydrogen bonds strength and geometry results from the symmetry of the molecule. Vibrational frequencies for AQ5H were computed to confirm the minimum energy structure and given in Table S7 in Supplementary Materials.

4.1.2. Chemical reactivity

Chemical reactivity descriptors were computed to explore the readability of anthraquinones to interact with DNA. The density of electrons on an atom is an important property that contains all the information about the molecular systems. Descriptors of chemical reactivity are good tools for predicting and understanding reactivity of compounds. These descriptors initially developed within the density functional theory framework.

Global quantities as chemical potential (μ), electronegativity (χ), chemical hardness (η), chemical softness (S), and electrophilicity (ω) of anthraquinones were calculated according to the equations presented elsewhere [42] and presented in Table 1. From the results in Table 1, it may be observed that the global softness decreases in the order AQ5 > AQ5H > 1,5-DAAQ. AQ5 has the highest global electrophilicity (7.312) and highest softness (0.439). Softness of a molecule is a measure of its polarizability and hence, its reactivity. In terms of softness, the reactivity of the anthraquinones goes in the order AQ5 > AQ5H > 1,5-DAAQ.

The calculated charge transfer ΔN between two systems *A* and *B* (the studied anthraquinones and DNA bases and DNA base pairs) was computed according to the equation [42–44]:

Table 1
Calculated global quantities: chemical potential (μ), electronegativity (χ), hardness (η), softness (**S**), and electrophilicity (ω) and charge transfer ΔN between the studied anthraquinones and DNA bases and base pairs.

	μ	χ	η	*S*	ω	E_{HOMO}	E_{LUMO}	$\Delta E_{L\text{-}H}$
AQ5	−4.082	4.082	1.140	0.439	7.312	−5.222	−2.943	2.279
AQ5H	−4.193	4.193	1.435	0.348	6.128	−5.628	−2.759	2.870
1,5-DAAQ	−4.349	4.349	1.537	0.325	6.150	−5.886	−2.811	3.075

	A	G	C	T	AT	GC
AQ5	−0.258	−0.744	−0.298	0.317	−0.546	−0.820
AQ5H	−0.508	−1.025	−0.539	0.111	−0.802	−1.085
1,5-DAAQ	−0.851	−1.367	−0.864	−0.215	−1.126	−1.385

ΔN is summarized in Table 1. Inspection of the calculated charge, as shown in the Table shows that the charge transfer takes place from DNA base pairs (AT and GC) to anthraquinones. The higher transferred charge with GC reflects the extent of interaction between anthraquinone and DNA base pair which is in agreement with our previous experimental studies [12]. AQ5 and AQ5H are electron acceptors to A, C, and G while they are electron donors toward T. 1,5-DAAQ has an electron accepting nature toward all

Table 2
Condensed Fukui Functions (f_k^0) (f_k^+) and (f_k^-) indices of AQ5.

	Fukui Indices for radical attack f_k^0		Fukui Indices for nucleophilic attack f_k^+		Fukui Indices for electrophilic attack f_k^-	
	Mulliken	Hirshfeld	Mulliken	Hirshfeld	Mulliken	Hirshfeld
C (1)	0.028	0.041	0.038	0.051	0.018	0.031
C (2)	0.028	0.036	0.022	0.030	0.034	0.042
C (3)	0.014	0.017	0.011	0.014	0.016	0.020
C (4)	0.015	0.016	0.006	0.010	0.025	0.023
C (5)	0.021	0.027	0.025	0.027	0.017	0.027
C (6)	0.029	0.043	0.033	0.049	0.025	0.037
C (7)	0.028	0.025	0.045	0.043	0.011	0.008
C (8)	0.016	0.017	0.005	0.010	0.026	0.024
C (9)	0.014	0.018	0.011	0.014	0.018	0.021
C (10)	0.027	0.025	0.044	0.043	0.01	0.008
C (11)	0.029	0.036	0.023	0.030	0.034	0.043
C (12)	0.026	0.041	0.037	0.051	0.016	0.030
C (13)	0.03	0.043	0.034	0.050	0.025	0.037
C (14)	0.019	0.027	0.023	0.027	0.016	0.027
O (15)	0.035	0.037	0.054	0.056	0.016	0.018
O (16)	0.036	0.038	0.055	0.056	0.016	0.019
O (17)	0.054	0.051	0.043	0.040	0.065	0.061
N (18)	0.045	0.045	0.029	0.031	0.062	0.060
C (19)	−0.019	0.008	−0.017	0.006	−0.021	0.010
C (20)	0.001	0.004	0.002	0.003	−0.001	0.006
N (21)	0.002	0.006	0.001	0.004	0.003	0.007
C (22)	−0.011	0.005	−0.01	0.005	−0.012	0.006
C (23)	−0.009	0.003	−0.008	0.002	−0.01	0.004
H (24)	0.046	0.025	0.049	0.028	0.043	0.022
H (25)	0.043	0.022	0.045	0.024	0.04	0.020
H (26)	0.046	0.025	0.049	0.028	0.043	0.022
H (27)	0.043	0.022	0.047	0.024	0.04	0.020
H (28)	0.015	0.014	0.015	0.013	0.015	0.015
H (29)	0.018	0.014	0.015	0.012	0.02	0.017
H (30)	0.02	0.010	0.017	0.009	0.023	0.012
H (31)	0.029	0.014	0.026	0.013	0.031	0.016
H (32)	0.011	0.005	0.009	0.004	0.013	0.005
H (33)	−0.002	0.001	−0.005	−0.001	0.002	0.002
H (34)	0.018	0.010	0.017	0.009	0.019	0.010
H (35)	0.007	0.004	0.006	0.003	0.008	0.004
H (36)	0.011	0.006	0.01	0.005	0.013	0.007
H (37)	0.021	0.010	0.02	0.010	0.022	0.011
H (38)	0.008	0.004	0.007	0.003	0.01	0.005
H (39)	−0.003	0.000	−0.003	−0.001	−0.002	0.000
O (40)	0.054	0.051	0.043	0.041	0.065	0.061
N (41)	0.045	0.045	0.029	0.031	0.061	0.059
C (42)	−0.019	0.008	−0.017	0.006	−0.02	0.010
C (43)	0.002	0.004	0.003	0.003	0.001	0.005
N (44)	−0.004	0.001	−0.004	0.001	−0.004	0.002
C (45)	−0.009	0.004	−0.008	0.004	−0.009	0.005
C (46)	−0.01	0.003	−0.009	0.003	−0.01	0.003
H (47)	0.015	0.014	0.015	0.013	0.015	0.015
H (48)	0.018	0.014	0.015	0.012	0.02	0.017
H (49)	0.027	0.013	0.025	0.012	0.029	0.014
H (50)	0.022	0.011	0.019	0.010	0.025	0.013
H (51)	−0.004	0.000	−0.006	−0.001	−0.002	0.000
H (52)	0.012	0.005	0.01	0.004	0.013	0.006
H (53)	0.018	0.009	0.017	0.009	0.018	0.009
H (54)	0.000	0.001	−0.001	0.000	0.001	0.001
H (55)	0.013	0.006	0.012	0.006	0.013	0.006
H (56)	0.018	0.009	0.018	0.009	0.019	0.010
H (57)	0.013	0.006	0.012	0.006	0.013	0.006
H (58)	0.000	0.001	0	0.001	0	0.001

Please cite this article in press as: J.S. Al-Otaibi, T.M. EL Gogary, Synthesis of novel anthraquinones: Molecular structure, molecular chemical reactivity descriptors and interactions with DNA as antibiotic and anti-cancer drugs, Journal of Molecular Structure (2016), http://dx.doi.org/10.1016/j.molstruc.2016.10.098

Table 3
Condensed Fukui Functions ((f_k^0) (f_k^+) and (f_k^-) indices of AQ5H.

	Fukui Indices for radical attack f_k^0		Fukui Indices for nucleophilic attack f_k^+		Fukui Indices for electrophilic attack f_k^-	
	Mulliken	Hirshfeld	Mulliken	Hirshfeld	Mulliken	Hirshfeld
C (1)	0.015	0.021	0.021	0.022	0.009	0.020
C (2)	0.015	0.015	0.005	0.011	0.024	0.019
C (3)	0.032	0.032	0.053	0.055	0.01	0.008
C (4)	0.012	0.019	0.02	0.024	0.004	0.015
C (5)	0.032	0.033	0.053	0.055	0.012	0.011
C (6)	0.016	0.017	0.003	0.011	0.03	0.024
C (7)	0.012	0.022	0.018	0.024	0.007	0.019
C (8)	0.038	0.047	0.037	0.049	0.039	0.046
C (9)	0.034	0.045	0.022	0.035	0.046	0.055
O (10)	0.052	0.052	0.079	0.079	0.025	0.025
C (11)	0.013	0.021	0.02	0.022	0.006	0.020
C (12)	0.036	0.048	0.022	0.035	0.05	0.060
C (13)	0.038	0.048	0.037	0.049	0.038	0.047
C (14)	0.015	0.037	0.025	0.047	0.005	0.028
O (15)	0.052	0.052	0.08	0.079	0.025	0.025
H (16)	0.044	0.024	0.047	0.025	0.041	0.022
H (17)	0.038	0.022	0.038	0.021	0.038	0.023
H (18)	0.047	0.025	0.05	0.028	0.043	0.022
N (19)	0.046	0.046	0.023	0.026	0.07	0.066
H (20)	0.018	0.015	0.014	0.011	0.022	0.019
C (21)	−0.02	0.009	−0.017	0.006	−0.023	0.012
H (22)	0.03	0.015	0.026	0.013	0.035	0.018
H (23)	0.022	0.011	0.017	0.008	0.027	0.013
C (24)	−0.001	0.006	0.002	0.002	−0.004	0.009
H (25)	0.001	0.003	−0.006	−0.001	0.008	0.006
H (26)	0.013	0.006	0.008	0.003	0.018	0.008
N (27)	0.008	0.012	0.001	0.003	0.015	0.020
C (28)	−0.012	0.006	−0.01	0.004	−0.015	0.009
H (29)	0.02	0.010	0.017	0.009	0.023	0.012
H (30)	0.015	0.008	0.01	0.005	0.02	0.011
H (31)	0.009	0.005	0.006	0.003	0.012	0.007
C (32)	−0.011	0.004	−0.008	0.002	−0.013	0.006
H (33)	0.023	0.011	0.02	0.010	0.025	0.013
H (34)	0.012	0.006	0.006	0.003	0.017	0.009
H (35)	0	0.001	−0.003	−0.001	0.002	0.002
H (36)	0.016	0.013	0.012	0.010	0.02	0.016
C (37)	0.015	0.037	0.025	0.047	0.005	0.028
H (38)	0.048	0.025	0.05	0.028	0.045	0.023
H (39)	0.043	0.023	0.047	0.025	0.04	0.021
H (40)	0.04	0.023	0.038	0.021	0.042	0.025
N (41)	0.042	0.043	0.024	0.026	0.061	0.060
C (42)	−0.001	0.002	0	0.001	−0.002	0.002
H (43)	0.008	0.003	0.006	0.002	0.01	0.004
H (44)	0.005	0.002	0.003	0.001	0.007	0.003
C (45)	−0.023	0.008	−0.02	0.006	−0.025	0.010
H (46)	0.025	0.013	0.021	0.010	0.029	0.015
H (47)	0.026	0.014	0.023	0.011	0.03	0.016
N (48)	−0.002	0.004	−0.003	0.002	0	0.006
C (49)	−0.01	0.004	−0.009	0.004	−0.011	0.005
H (50)	0.017	0.009	0.016	0.008	0.017	0.009
H (51)	0.012	0.006	0.01	0.005	0.013	0.007
H (52)	0.006	0.003	0.005	0.003	0.007	0.004
C (53)	−0.007	0.003	−0.007	0.003	−0.008	0.004
H (54)	0.012	0.006	0.01	0.005	0.014	0.007
H (55)	0.018	0.009	0.017	0.008	0.019	0.009
H (56)	−0.004	0.000	−0.004	−0.001	−0.003	0.000

Table 4
Condensed Fukui Functions (f_k^0) (f_k^+) and (f_k^-) indices of 1,5-DAAQ.

	Fukui Indices for radical attack f_k^0		Fukui Indices for nucleophilic attack f_k^+		Fukui Indices for electrophilic attack f_k^-	
	Mulliken	Hirshfeld	Mulliken	Hirshfeld	Mulliken	Hirshfeld
C (1)	0.018	0.041	0.027	0.049	0.008	0.033
C (2)	0.041	0.053	0.024	0.038	0.057	0.068
C (3)	0.012	0.023	0.018	0.025	0.006	0.021
C (4)	0.019	0.019	0.006	0.013	0.032	0.026
C (5)	0.013	0.026	0.017	0.024	0.008	0.029
C (6)	0.04	0.053	0.038	0.052	0.042	0.055
C (7)	0.035	0.034	0.057	0.057	0.013	0.011
C (8)	0.018	0.019	0.005	0.013	0.031	0.025
C (9)	0.013	0.023	0.018	0.025	0.008	0.021
C (10)	0.034	0.034	0.056	0.057	0.012	0.011
C (11)	0.013	0.026	0.017	0.024	0.009	0.029
C (12)	0.041	0.053	0.039	0.052	0.043	0.054
C (13)	0.016	0.041	0.026	0.049	0.007	0.033
C (14)	0.039	0.053	0.023	0.038	0.055	0.067
O (15)	0.057	0.057	0.084	0.083	0.03	0.03
O (16)	0.057	0.057	0.084	0.083	0.03	0.031
N (17)	0.054	0.059	0.028	0.035	0.08	0.082
H (18)	0.053	0.029	0.054	0.031	0.052	0.027
H (19)	0.045	0.026	0.042	0.023	0.049	0.029
H (20)	0.054	0.030	0.054	0.030	0.054	0.029
H (21)	0.054	0.030	0.055	0.031	0.054	0.029
H (22)	0.053	0.029	0.054	0.031	0.052	0.027
H (23)	0.023	0.020	0.018	0.015	0.027	0.025
H (24)	0.038	0.029	0.034	0.024	0.042	0.034
N (25)	0.054	0.059	0.028	0.035	0.081	0.083
H (26)	0.045	0.026	0.042	0.023	0.048	0.029
H (27)	0.023	0.020	0.018	0.015	0.028	0.025
H (28)	0.038	0.029	0.034	0.024	0.042	0.035

bases and base pairs. Comparing AQ5 and AQ5H with 1,5-DAAQ confirm that the order of interaction, taking the amount of charge transferred as a measure of interaction strength, is 1,5-DAAQ > AQ5H > AQ5. Values of ΔN, as shown in Table 1 clearly, confirm the importance of the charge transfer mechanism for the course of drug/DNA interaction.

Fukui [45] introduced a qualitative approach of chemical reactivity in the form of what we call Frontier Orbital Theory. Later, this theory was demonstrated [46,47] in the framework of DFT. In a molecular system, the atomic site, which possesses highest condensed Fukui function, favors the higher reactivity. Tables 2–4 show the condensed Fukui functions and local softness as calculated based on Mullikin and Hirchfeld charges for AQ5, AQ5H and 1,5-DAAQ. Isosurface maps for Fukui functions of electrophilic, nucleophilic and radical attack are given in Fig. 2. Isosurface maps show that AQ5 acts better as nucleophilic and free radical attack than electrophilic attack. Ring system in AQ5 has no electrophilic centers, these centers are shown on oxygen and nitrogen atoms. On the other hand, nucleophilic and free radical attack are shown on the ring system. From the results of Table 2, the reactivity for the radical attack was found on C1, C6, C11, C12, C13, O15, O16, O17, N18, O40 and N41. Among these atoms the reactivity of radical attack could be ranked as N17 = O40 > N41 = N18 > C6 = C13 > C12 = C1 > O16 > O15. For nucleophilic attack, the most reactive sites are O15 and O16 (0.056). The order of reactivity toward nucleophilic attack could be ranked as O16 = O15 > C1 = C12 > C13 > C1 > C6 > C7 = C10 > N18. On the other hand, for electrophilic attack, the most reactive site is O17(0.061), N40(0.061), N18(0.060) and N41(0.059). The reactivity order toward electrophilic attack could be ranked as N40 = O17 > N18 > N41 > C11 > C2 > C6=C13 > C1 > C5=C14 > C8 > C9. From Table 3, it is clear that AQ5H is more reactive than AQ5 when comparing values (Mullikin and Hirshfeld) of condensed Fukui functions for electrophilic and nucleophilic attack as shown, also, from Fig. 2. For electrophilic attack, the highest Fukui function value is accommodated on N19 (0.066). the order of the electrophilic attack is N19 (0.066) > N42 = C12 (0.060) > C9 (0.055) > C13 (0.047) > C8 (0.046). For nucleophilic attack the most nucleophilic site is O15 (Fukui function value is 0.079) and the tendency for nucleophilic attack decreases as O15 (0.079) > C3=C5 (0.055) > C8=C13 (0.049) > C14 = C37 (0.047). AQ5H has larger tendency for nucleophilic attack (0.079 on O19) than AQ5 (0.056 on O15). For free radical attack, there are many reactive sites with

Please cite this article in press as: J.S. Al-Otaibi, T.M. EL Gogary, Synthesis of novel anthraquinones: Molecular structure, molecular chemical reactivity descriptors and interactions with DNA as antibiotic and anti-cancer drugs, Journal of Molecular Structure (2016), http://dx.doi.org/10.1016/j.molstruc.2016.10.098

moderate Fukui function values. The susceptibility of the free radical attack decreases as O15 (0.052) > C12 = C13 (0.048) > C8 (0.047) > N19 (0.046) > C9 (0.045) > C14 = C37 (0.037) > C5 (0.033). For 1,5-DAAQ (Table 4), the free radical reactivity decreases in the order, N17 = N25 (0.059) > O15 = O16 (0.057) > C2=C6=C12 = C14 (0.053) > C1=C13 (0.041) >C7=C10 (0.034). The tendency for nucleophilic attack in 1,5-DAAQ decreases as O15 = O16 (0.083) > C7=C10 (0.057) > C6=C12 (0.052) > C1=C13 (0.049) > C2 0.038) > N17 = N25 (0.035). The most electrophilic site is O17and O40 and the order decreases as O17 = O40 (0.061) > N18 (0.060) > N41 (0.059) > C11 (0.043) >C2 (0.042) > C6 (0.037).

4.2. Frontier orbital analysis

Highest occupied molecular orbital (HOMO) and lowest unoccupied molecular orbital (LUMO) for AQ5, AQ5H and 1,5-DAAQ are calculated and presented in Fig. 3. HOMO and LUMO, as frontier molecular orbitals, are considered as very important molecular parameters for the stability and chemical reactivity of the species [48,49]. HOMO and LUMO energies, and LUMO−HOMO energy gap (ΔE_{L-H}), in eV, are displayed in Table 1. The lower the HOMO energy the more readily of that orbital to participate in chemical reaction by donating electrons. LUMO energy, on the other hand, determine the ability to accept an electron in a chemical change. LUMO−HOMO energy gap reflects the chemical hardness−softness and polarizability of the molecule and hence its biological activity [50,51].

The energy values of HOMO are computed as −5.222, −5.628 and −5.886 eV and LUMO are −2.943, −2.759 and −2.811 eV, and the energy gap values are 2.279, 2.870 and 3.075 eV for AQ5, AQ5H and 1,5-DAAQ, respectively. Computed values of ΔE_{L-H} shows that AQ5 is more reactive than AQ5H which is more reactive than 1,5-DAAQ. This is in accord with the calculated chemical softness 0.439, 0.348 and 0.325 for AQ5, AQ5H and 1,5-DAAQ respectively.

Anthraquinones are electron acceptors toward DNA bases and base pair as appeared from the computed ΔN negative values in Table 1. So that, the anthraquinones LUMO energy is the determining factor in their interaction with DNA and hence, the order of reactivity of these anthraquinones with DNA could be ranked as 1,5-DAAQ > AQ5H > AQ5. This is consistent with values of calculated charge transfer ΔN of −0.546, −0.802, and −1.126 for AQ5, AQ5H and 1,5-DAAQ respectively toward AT base pair and −0.820, −1.085 and −1.385 toward GC base pair.

HOMO and LUMO plots of AQ5, AQ5H and 1,5-DAAQ are presented in Fig. 3. As can be seen in Fig. 3, the HOMO of AQ5 is delocalized mainly on the carbon C−C bonds, OH and NH(R) groups. Carbonyl groups and C−H bonds show anti-bonding nature where no electron projection at these regions. LUMO of AQ5 is being participated mainly from the ring carbons and oxygen atoms of the C═O and O−H groups. It is clear from Fig. 3 that, the LUMO of AQ5 shows antibonding character over the C−H bonds both in the ring and side chain.

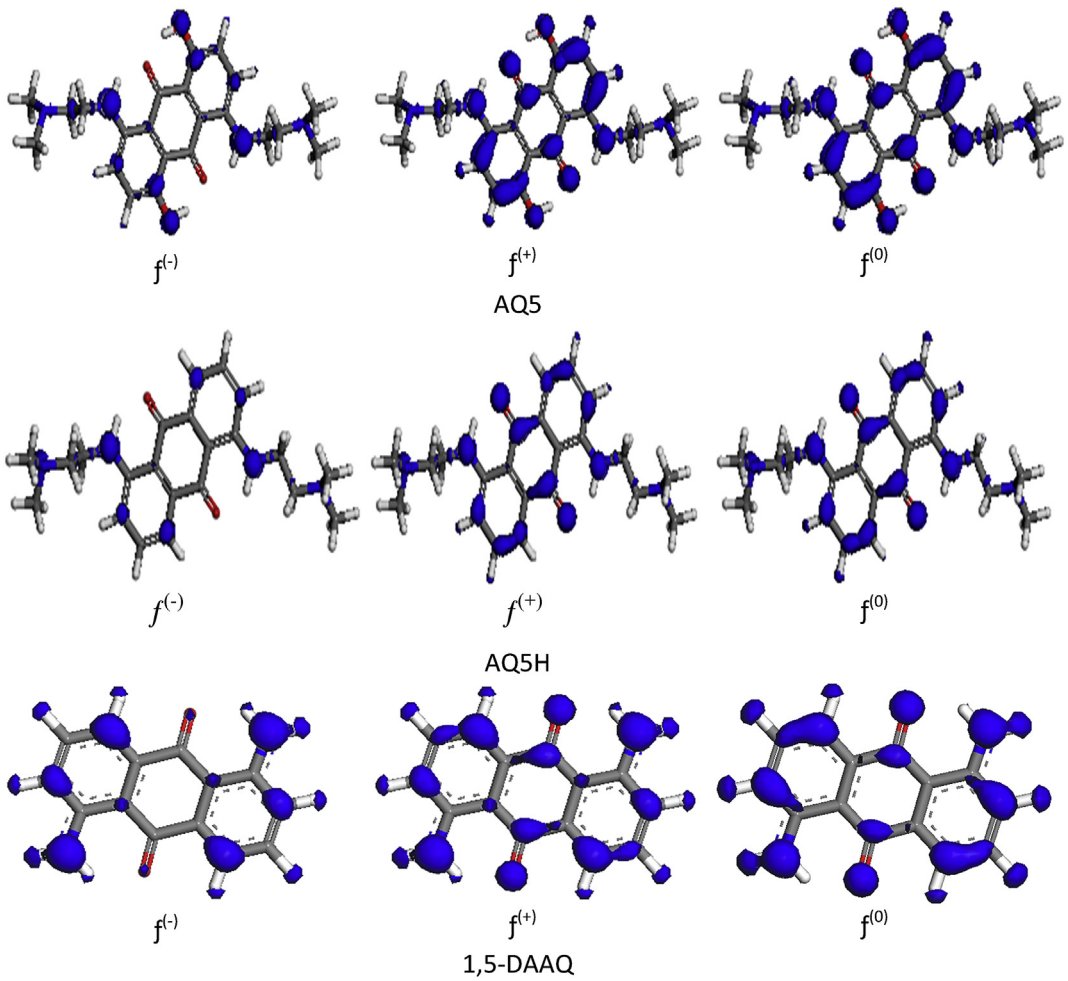

Fig. 2. Isosurface maps for Fukui functions of electrophilic, nucleophilic and radical attack for AQ5, AQ5H and 1,5-DAAQ.

Please cite this article in press as: J.S. Al-Otaibi, T.M. EL Gogary, Synthesis of novel anthraquinones: Molecular structure, molecular chemical reactivity descriptors and interactions with DNA as antibiotic and anti-cancer drugs, Journal of Molecular Structure (2016), http://dx.doi.org/10.1016/j.molstruc.2016.10.098

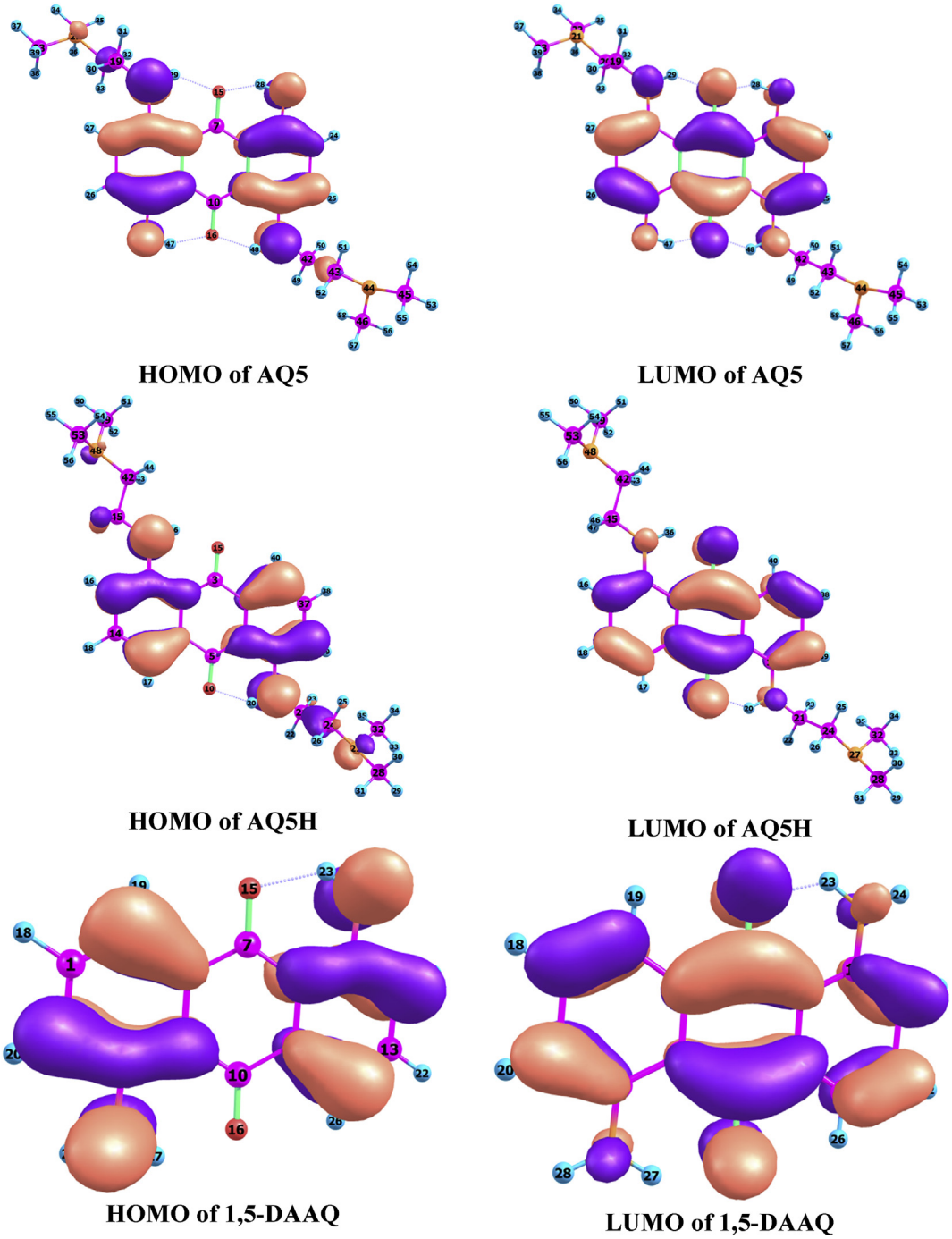

Fig. 3. HOMO and LUMO plots of AQ5, AQ5H and 1,5-DAAQ.

The HOMO of AQ5H is delocalized on the ring carbon atoms except the carbonyl carbons and carbons meta to the side chain which show anti-bonding character. LUMO of the AQ5H is distributed on the ring system and the carbonyl oxygen. Both side chains show anti-bonding nature.

The HOMO of 1,5-DAAQ is delocalized on the amino groups and terminal ring carbon atoms except the carbons located meta to the amino group. Carbonyl carbons and C—H bonds show anti-bonding character. The LUMO are delocalized on the ring carbons and oxygen and nitrogen atoms. C—H bonds show anti-bonding character.

4.3. Experimental study

The anthraquinone drug/DNA intercalation complexes have been investigated using different experimental techniques [52–54] including NMR spectroscopy [55,56] and modeled using computational quantum chemistry [21,57–59].

In this work the anthraquinone drug/DNA interactions have been discussed. Three types of DNA were used, namely calf thymus DNA, polydeoxyadenylic acid-polythymidylic acid (Poly[dA].Poly[dT]) and polydeoxyguanylic acid-polydeoxycytidylic acid (Poly[dG].Poly[dC]). AQ5 and AQ5H were experimentally investigated

Please cite this article in press as: J.S. Al-Otaibi, T.M. EL Gogary, Synthesis of novel anthraquinones: Molecular structure, molecular chemical reactivity descriptors and interactions with DNA as antibiotic and anti-cancer drugs, Journal of Molecular Structure (2016), http://dx.doi.org/10.1016/j.molstruc.2016.10.098

Table 5
^{1}H NMR chemical shift differences, Δ (Hz) for different drug protons in their mixtures with DNA.

System	Drug: DNA	$N(CH_3)_2$		$ArHNCH_2$		Ar[a]	
		Δ	Broadening	Δ	Broadening	Δ	Broadening
AQ5/calf thymus	1:0.5	−0.16	–	−0.13	–	1.89	–
	1:1	−0.05	–	−0.37	–	2.46	–
AQ5H/calf thymus	1:0.25	−0.29	✓	1.19	✓	7.99	✓
						12.02	
						6.76	
	1:0.5	−0.21	✓	too broad	✓	too broad	✓
AQ5/P(dA).P(dT)	1:0.25	−0.03	–	−0.52	–	2.27	–
	1:0.5	−0.20	–	−6.62	–	3.38	–
AQ5H/P(dA).P(dT)	1:0.25	−0.27	✓	0.54	✓	3.69	✓
						5.54	
						2.97	
	1:0.5	–	✓	−0.22	✓	7.73	✓
						10.11	
						8.02	
AQ5/P(dG).P(C)	1:0.5	−0.61	–	−0.15	–	5.61	–
	1:1	−0.68	–	0.08	–	1.63	–
AQ5H/P(dG).P(C)	1:0.25	−0.18	✓	−0.11	✓	1.21	✓
						2.60	
						0.74	
	1:0.5	−0.30	✓	−0.15	✓	1.5	✓
						3.24	
						0.90	

[a] Aromatic protons in AQ5 exhibit identical shifts. For AQ5H the shifts for protons at positions 2&6, 3&7 and 4&8 are presented sequentially.

while the low solubility of 1,5-DAAQ does not allow such investigation. This study has been done using NMR and UV–VIS spectroscopy.

4.4. NMR studies

The NMR spectra of drug/DNA mixtures were obtained in D_2O buffer at pH = 7.2 in different drug/DNA ratios. Different drug NMR signals in the spectra of drug/DNA mixtures were compared with that of the corresponding drug in its pure solution. Generally two observations were obtained, the first is the peak shift and the second is the peak broadening. NMR spectra of AQ5 and AQ5H, with calf thymus DNA, (Poly[dA].Poly[dT]) and (Poly[dG].Poly[dC]) were obtained in D_2O buffer at pH = 7.2 in different drug/DNA ratios at 30 °C in presence of TMS as an internal standard. Table 5 gives the degree of peak shift (in Hz, defined as (chemical shift unbound)-(chemical shift bound)) and the presence of the broadening for different drug/DNA ratios of the studied drugs with different DNA. Delta shift value would show the change in the electronic environment compared to unbound.

The chemical shifts of proton environments in the AQs were observed to change upon interaction with DNA (Table 5). These shifts can be interpreted in terms of the mode of binding and the orientation of the complexed species. Interaction with DNA through charge transfer complex formation will place electron density within the LUMO of the acceptor, and the change in chemical shift (Δ) for a given environment should relate closely to its position within the LUMO. Conversely, if there is no apparent link between the chemical shift changes and positions of the different environments within the LUMO, then a non charge transfer stacking interaction is the most likely mode of binding. Here the extent of the chemical shift change (Δ) is dependant on the strength of the interaction and on the electronics of the environment within the drug/DNA. For AQ5/DNA and AQ5H/DNA, all proton environments are significantly altered. The smallest values of Δ are observed for the equivalent proton positions 1,4,5 and 8. The close correlation between Δ and LUMO density indicates that charge transfer is the principle mode of binding in this complex. Fig. S1 in the Supplementary Materials represents the H NMR spectra of AQ5 and AQ5/P(dG).P(dC) showing the broadening of the methyl peak.

Different drug NMR signals in the spectra of drug/calf thymus DNA mixtures were compared with that of the corresponding drug in its pure solution. It was observed that the side chain protons were always shifted downfield whereas the aromatic protons show up-field shift, except for drug/calf thymus. Aromatic protons show more shift (Δ ≈ 1.00–12.00) than side chain protons (Δ ≈ −0.03: −7.00). This indicates that the mode of interaction is intercalation in nature. The intercalated ring system interacts more effectively with the DNA bases. The methyl protons $N(CH_3)_2$ of AQ5H (≈−0.21: −0.29) is more shifted than that of AQ5 (≈−0.03: −0.20). The hydroxyl groups of the intercalated drug in AQ5 form intermolecular hydrogen bonding that leads to locating of the N(CH3)2 outside the interaction zone hence lower shift is observed. In case of intercalated AQ5H the $N(CH_3)_2$ group is present within the interaction site which results in higher shift. Another interesting observation is the peak broadening which depends on

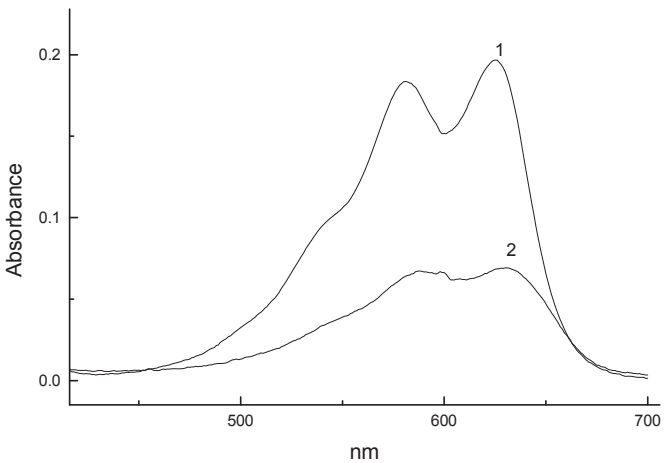

Fig. 4. The electronic absorption spectra of 1) free AQ5H ([AQ5H] = 1.379 × 10^{-5} M), 2) AQ5H/p(dG).p(dC) complex ([AQ5H] = 6.435 × 10^{-6} M, [DNA] = 1.760 × 10^{-4} M).

Please cite this article in press as: J.S. Al-Otaibi, T.M. EL Gogary, Synthesis of novel anthraquinones: Molecular structure, molecular chemical reactivity descriptors and interactions with DNA as antibiotic and anti-cancer drugs, Journal of Molecular Structure (2016), http://dx.doi.org/10.1016/j.molstruc.2016.10.098

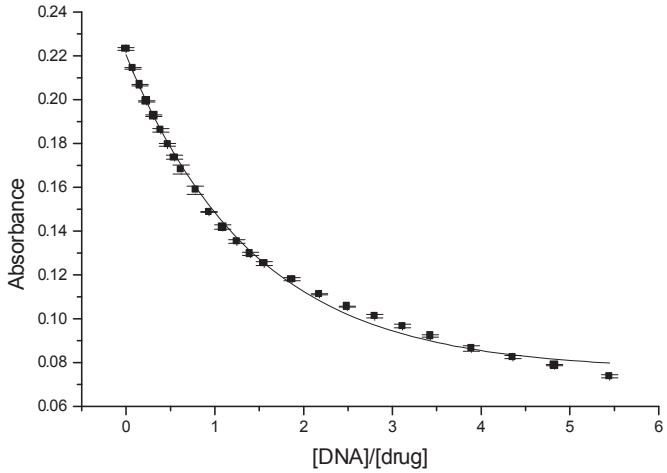

Fig. 5. Absorbance at 598 nm of the system AQ5H/P(dG).P(dC) against [DNA]/[drug] ratio. Uncertainity in absorbance values is displayed. Solid line shows a theoretical curve based on the best fit of the absorbance data to the first order exponential decay function.

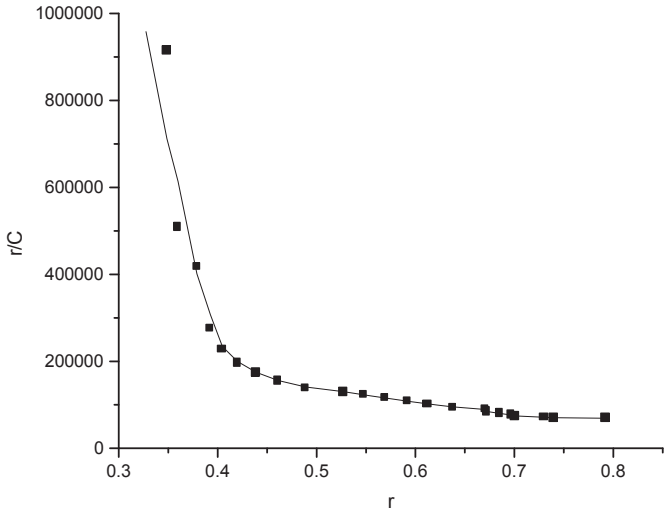

Fig. 6. Scatchard plot of AQ5H bound to P(dG).P(dC). Solid line shows a theoretical curve based on smoothing to adjacent averaging.

the drug/DNA ratio. The degree of broadening increases with increasing of DNA concentration. At high DNA concentration the drug peaks are too broad to be seen at all. On the other hand, at low DNA concentration there is an equilibrium between the bound and the free drug, and an average-positioned signal was observed.

The order of shift of the aromatic and side chain protons of AQ5 and AQ5H is P(dG).P(dC) < P(dA).P(dT). The shift in the aromatic protons of 6&7 positions is larger than that of protons of 2&3. The magnitude of the shift of the protons of AQ5 and AQ5H suggests that these drugs are AT selective, which is consistent with the results from the spectrophotometric titration as shown below. Considering the magnitude of the shift as a measure of the drug/DNA interaction, AQ5H shows stronger interaction than AQ5 as can be seen from Table 5. This result is consistent with the results of the computed charge transfer of AT and GC as shown above (Table 1).

4.5. UV–VIS studies

The interactions between three types of DNA (calf thymus DNA, (Poly[dA].Poly[dT]) and, (Poly[dG].Poly[dC])) and anthraquinone drugs (AQ5 and AQ5H) were investigated in Tris buffer at pH = 7.2 by absorption spectroscopy.

The absorption spectra of AQ5 and AQ5H with DNA were obtained in Tris buffer at the physiological pH in different drug/DNA ratios at room temperature. Fig. 4 shows the absorption spectra of AQ5H/p(dG).p(dC) system as an example. Similar spectra were obtained for other systems. As can be seen from the spectra the changes in the uv–vis spectra induced by excess amounts of DNA to the drug solution, show hypochromicity in the absorbance of the drug. Furthermore, a shift to higher wavelength was also observed as compared to the free drug. The degree of the red shift (in nm) is 16, 16, 17, 11, 7, 10 nm for AQ5/calf thymus DNA, AQ5/p(dA).p(dT), AQ5/p(dG).p(dC), AQ5H/calf thymus DNA, AQ5H/p(dA).p(dT), and AQ5H/p(dG).p(dC) respectively. Table S8 in Supplementary Material gives the degree of the red shift (in nm) observed in the spectra of the drugs with DNA. The modifications of these absorption spectra are common features of drugs upon binding to DNA due to strong interactions between the electronic states of the DNA bases with the drug [60]. This leads to an electronic redistribution of the bound drug, leading usually to spectral changes (red-shifts and hypochromicity) [61,62].

The absorption titration data for these drugs with DNA were employed to calculate the affinity constants and number of base pairs occupied by a bound drug molecule. The experiments were done in triplicates to estimate the uncertainity in the measured parameters. Fig. 5 shows the uncertainity (as a standard deviation) in the absorbance values at 598 nm against DNA/drug ratio for the system AQ5H/p(dG).p(dC). The absorbance titration data for the drugs bound to DNA were analyzed according to the MC Ghee and Von Hippel model [63] and plotted as a Scatchard representation. Fig. 6 shows the Scatchard plot for the binding of AQ5H/p(dG).p(dC).

The curvature of the Scatchard plot is a confirmation of the presence of two types of binding modes of the drug to DNA, i.e. intercalation and surface binding. The data points in the Scatchard plots can be divided into two portions and treated separately to determine the binding parameters for each mode of binding. The least squares method was used to fit the data points (linearly) of each data point portion of the Scatchard plot. Affinity constants (K)

Table 6
Affinity constants (K)[a] and numbers of base pairs bound per drug molecule (n)[b] for the binding of AQs drugs with DNA.

Drug/DNA	K_1	n_1	K_2	n_2
AQ5/calf thymus	$2.8 \times 10^7 \pm 5 \times 10^5$	14.29 ± 0.002	$6.3 \times 10^5 \pm 1.\ x10^3$	8.33 ± 0.0
AQ5H/calf thymus	$2.1 \times 10^7 \pm 1.2 \times 10^6$	10.0 ± 0.001	$1.7 \times 10^5 \pm 2.8 \times 10^3$	2.86 ± 0.04
AQ5/P(dA).P(dT)	$3.0 \times 10^7 \pm 2.4 \times 10^4$	10.00 ± 0.000	$7.3 \times 10^4 \pm 11314$	0.90 ± 0.16
AQ5H/P(dA).P(dT)	$7.1 \times 10^6 \pm 1.4 \times 10^5$	5.73 ± 0.001	$4.2 \times 10^5 \pm 22243$	4.20 ± 0.005
AQ5/P(dG).P(dC)	$1.39 \times 10^7 \pm 1.6 \times 10^6$	2.5 ± 0.001	$3.3 \times 10^5 \pm 50968$	1.1 ± 0.07
AQ5H/P(dG).P(dC)	$6.0 \times 10^6 \pm 1.4 \times 10^6$	10.0 ± 0.002	$4.7 \times 10^5 \pm 5364$	5.9 ± 0.002

[a] K_1 intercalation binding affinity constant, K_2 surface binding affinity constant.
[b] n_1 number of drug molecules intercalated per base pair, n_2 number of drug molecules surface binding per base pair.

Please cite this article in press as: J.S. Al-Otaibi, T.M. EL Gogary, Synthesis of novel anthraquinones: Molecular structure, molecular chemical reactivity descriptors and interactions with DNA as antibiotic and anti-cancer drugs, Journal of Molecular Structure (2016), http://dx.doi.org/10.1016/j.molstruc.2016.10.098

and number of base pairs occupied by a bound drug molecule (n) were calculated from the slope and the intercept with the X-axis, respectively, and are displayed in Table 6 where K_1 and n_1 are for intercalation mode and K_2 and n_2 for surface binding mode. In order of decreasing intercalation affinity constant of the drugs to all types of DNA, the drugs ranked as follows: AQ5 > AQ5H. This result is consistent with the measured red shift in the UV–VIS spectra of the drug/DNA solutions as shown in Table S8 in the Supplementary Material. However, in order of decreasing surface binding affinity constant of the drugs to calf thymus DNA the drugs ranked as follows: AQ5H > AQ5. AQ5/P(dA).P(dT) shows the most stable complex ($3.0 \times 10^7\ M^{-1}$). AQ5 shows largest tendency and selectivity to AT sites. This is consistent with the NMR investigations which show highest chemical shift with P(dA).P(dT) as displayed in Table 5. However, this result is inconsistent with the calculated charge transfer ΔN (Table 1) which shows that highest charge transfer, ΔN, was found with GC. Affinity constants for surface binding ($\approx 7-73 \times 10^4\ M^{-1}$) are much smaller than that of the intercalation binding ($\approx 0.6-3.0 \times 10^7\ M^{-1}$). Surface binding affinity constants values are comparable with that measured elsewhere [1,2]. On the other hand, the measured intercalation affinity constants suggest strong drug/DNA interaction which are much more than that measured for flavonoid/DNA intercalation [64,65]. A value of n is measured as 2.5 (Table 6) was observed only for the system AQ5/P(dG).P(dC) which is in the range typically observed for DNA intercalators.

5. Conclusion

AQ5 and AQ5H were synthesized and confirmed. Anthraquinone DNA affinic agents AQ5, AQ5H and 1,5-DAAQ were investigated computationally and experimentally to explore their potency as anti-cancer drugs. According to the computational studies at B3LYP/6-31 + G(d) level four conformers of AQ5 were identified within the range of total energy difference, ΔE, 42 kcal/mol due to intra molecular hydrogen bonding. Values of computed Fukui functions for nucleophilic attack prove the higher susceptibility of these anthraquinones for nucleophilic attack. The calculated charge shows that the charge transfer takes place from DNA base pairs (AT and GC) to anthraquinones. The higher transferred charge with GC reflects the extent of interaction between anthraquinone and DNA base pair which is in agreement with our previous experimental studies [12]. Values of the calculated charge indicate the predominance of the charge transfer mechanism for the course of drug/DNA interaction. NMR investigation of the drug/DNA solutions shows ^{1}HNMR peak shift and broadening which are proportional to drug:DNA ratio. The extent of the ^{1}HNMR peak shifts suggests that, these anthraquinones are AT selective and proves the predominance of the intercalation mode of interaction with respect to surface binding. These results were also confirmed by UV–VIS spectrophotometric DNA titration (Table 6). UV–VIS studies prove the presence of two binding modes namely intercalation and surface binding as shown from the curvature of the Schatchard plot. UV–VIS spectrophotometric DNA titration studies show hypochromicity and red shifts upon interaction.

Acknowledgement

This work was supported by the Deanship of Scientific Research, Princess Nourah Bint Abdul Rahman University.

Appendix A. Supplementary data

Supplementary data related to this article can be found at http://dx.doi.org/10.1016/j.molstruc.2016.10.098.

References

[1] H. Zollinger, Color Chemistry, Syntheses, Properties and Applications of Organic Dyes and Pigments, third ed., Wiley-VCH, Weinheim, 2003.
[2] F.J. Green, The Sigma–Aldrich Handbook of Stains, Dyes and Indicators, Aldrich Chemical Company Inc, Milwaukee, Wisconsin, 1990.
[3] L. Salmon-Chemin, E. Buisine, V. Yardley, S. Kohler, M.-A. Debreu, V. Landry, C. Sergheraert, S. Croft, R. Krauth-Siegel, E. Davioud-Charvet, J. Med. Chem. 44 (4) (2001) 548.
[4] O. Weigenand, A. Hussein, N. Lall, J. Meyer, J. Nat. Prod. 67 (11) (2004) 1936.
[5] H. Bai, S. Li, F. Yin, L. Hu, J. Nat. Prod. 68 (8) (2005) 1159.
[6] J. Malerich, T. Maimone, G. Elliott, D. Trauner, J. Am. Chem. Soc. 127 (19) (2005) 6276.
[7] P. Cai, F. Kong, M. Ruppen, G. Glasier, G. Carter, J. Nat. Prod. 68 (12) (2005) 1736.
[8] M.C. Cardia, M. Belgala, A. Delogu, E. Maccioni, II Farm. 56 (5) (2001) 49–54.
[9] G.-Z. Jin, Y.-J. You, Y. Kim, N.-H. Nam, B.-Z. Ahn, Eur. J. Med. Chem. 36 (2001) 1–6.
[10] B.-L. Wei, S.-H. Wu, M.-I. Chung, S.-J. Won, C.-N. Lin, Eur. J. Med. Chem. 35 (10) (2000) 89–98.
[11] E. Apostolova, S. Krumova, N. Tuparev, M.T. Molina, T.S. Filipova, I. Petkanchin, Colloids Surf. B Biointerfaces 29 (2003) 1–12.
[12] T.M. EL-Gogary, E. EL-Gendy, Spectrochem. Acta-A 59 (2003) 2635–2644.
[13] F. Tavakolinia, T. Baghipour, Z. Hossaini, D. Zareyee, M.A. Khalilzadeh, M. Rajabi, Nucleic Acid. Ther. 22 (4) (2012) 265–270.
[14] M. Rajabi, P. Signorelli, E. Gorincioi, R. Ghidoni, E. Santaniello, DNA Cell Biol. 29 (11) (2010) 687–691.
[15] S.L. Cravens, A.C. Navapanich, B.H. Geierstanger, D.C. Tahmassebi, T.J. Dwyer, J. Am. Chem. Soc. 132 (2010) 17588–17598.
[16] M. Rettig, W. Langel, A. Kamal, K. Weisz, Org. Biomol. Chem. 8 (2010) 3179–3187.
[17] I. Haq, Arch. Biochem. Biophys. 403 (2002) 1–15.
[18] A. Brown, Int. J. Mol. Sci. 10 (2009) 3457–3477.
[19] V. Ball, C. Maechling, Isothermal microcalorimetry to investigate non specific interactions in biophysical chemistry, Int. J. Mol. Sci. 10 (2009) 3283–3315.
[20] R. Strawn, T. Stockner, M. Melichercik, L. Jin, W.-F. Xue, J. Carey, R. Ettrich, Methods Enzymol. 492 (2011) 151–188.
[21] J.S. Al-Otaibi, P. Teesdale Spittle, T.M. EL Gogary, J. Mol. Struct. 1127 (2017) 751–760, http://dx.doi.org/10.1016/j.molstruc.2016.08.007.
[22] D.K. Palit, H. Pal, T. Mukherjee, J.P. Mittal, J. Chem. Soc. Faraday Trans. 86 (1990) 3861.
[23] J.P. Rasimas, G.J. Blanchard, J. Phys. Chem. 99 (1995) 11333.
[24] T. Yatsuhashi, H. Inoue, J. Phys. Chem. A 101 (1997) 8166.
[25] H. Inoue, M. Hida, N. Nakashima, K. Yoshihara, J. Phys. Chem. 86 (1982) 3184.
[26] S.R. Flom, P.F. Barbara, J. Phys. Chem. 89 (1985) 4489.
[27] H. Pal, D.K. Palit, T. Mukherjee, J.P. Mittal, Radiat. Phys. Chem. 40 (1992) 529.
[28] E.J. Land, T. Mukherjee, A.J. Swallow, J.M. Bruce, J. Chem. Soc. Faraday Trans. I 79 (1983) 391.
[29] H. Pal, D.K. Palit, T. Mukherjee, J.P. Mittal, J. Chem. Soc. Faraday Trans. 87 (1991) 1109.
[30] E. McAlpine, R.S. Sinclair, T.G. Truscott, E.J. Land, J. Chem. Soc. Faraday Trans. I 74 (1978) 597.
[31] D.K. Palit, H. Pal, T. Mukherjee, J.P. Mittal, J. Photochem, Photobiol. A Chem. 52 (1990) 375.
[32] H. Pal, D.K. Palit, T. Mukherjee, J.P. Mittal, J. Photochem, Photobiol. A Chem. 62 (1991) 183.
[33] J. Ritter, H.-U. Brost, T. Lindner, M. Hauser, S. Brosig, K. Bredereck, U.E. Steiner, D. Kuhn, J. Kelemen, H.E.A. Kramer, J. Photochem, Photobiol. A Chem. 41 (1988) 227.
[34] A.J. Carmichael, P. Riesz, Arch. Biochem. Biophys. 237 (1985) 433.
[35] Denny, William Alexander; Lee, Ho Huat, Preparation of 1,4-bis[[2-(dimethylamino)ethyl]amino]-5,8-dihydroxyanthracene-9,10-dione via 3,6-dichlorophthalic anhydride, PCT Int. Appl. (2000), WO 2000005194 A1 20000203.
[36] A.P. Krapcho, Z. Getahun, K.L. Avery Jr., J.K. Vargas, M.P. Hacker, S. Spinelli, G. Pezzoni, C. Manzotti, J. Med. Chem. 34 (8) (1991) 2373–2380.
[37] K.C. Murdock, R.G. Child, P.F. Fabio, R.D. Angier, R.E. Wallace, F.E. Durr, R.V. Citarella, J. Med. Chem. 22 (9) (1979) 1024–1030.
[38] M.J. Frisch, et al., Gaussian 09, Revision A.02, Gaussian, Inc., Wallingford CT, 2009.
[39] B. Delley, J. Chem. Phys. 92 (1990) 508.
[40] B. Delley, J. Chem. Phys. 113 (2000) 7756.
[41] Accelrys Software Inc, Material Studio Modeling Environment, Release v7.0, Accelrys Software Inc., San Diego, 2013.
[42] R. Parthasarathi, J. Padmanabhan, V. Subramanian, B. Maiti, P.K. Chattaraj, J. Phys. Chem. A 107 (48) (2003) 10346–10352.
[43] R.G. Parr, R.G.J. Pearson, Am. Chem. Soc. 105 (1983) 7512.
[44] R. Parthasarathi, J. Padmanabhan, U. Sarkar, B. Maiti, V. Subramanian, P. Kumar, J. Mol. Des. 2 (12) (2003) 798–813.
[45] K.J. Fukui, Chem. Phys. 20 (1952) 722, 22 (1954) 1433.
[46] R.G. Parr, W. Yang, J. Am. Chem. Soc. 106 (1984) 4049.
[47] W. Yang, R.G. Parr, Proc. Natl. Acad. Sci. U. S. A. 82 (1985) 6723.
[48] S. Gunasekaran, R.A. Balaji, S. Kumeresan, G. Anand, C.S. Srinivasan, J. Anal. Sci. Spectrosc. 53 (2008) 149–162.

Please cite this article in press as: J.S. Al-Otaibi, T.M. EL Gogary, Synthesis of novel anthraquinones: Molecular structure, molecular chemical reactivity descriptors and interactions with DNA as antibiotic and anti-cancer drugs, Journal of Molecular Structure (2016), http://dx.doi.org/10.1016/j.molstruc.2016.10.098

[49] J.R. Durig, T.S. Little, T.K. Gounev, J.K. Gardner, J.F. Sullivan, J. Mol. Struct. 375 (1) (1996) 83–94.
[50] B. Kosar, C. Albayrak, Spectrochim. Acta. A 78 (2011) 160–167.
[51] D. Sajan, K.U. Lakshmi, Y. Erdogdu, I.H. Joe, Spectrochim. Acta. A. 78 (2011) 113–121.
[52] A.P. Krapcho, J.J. Landi, K.J. Shaw, D.G. Phinney, M.P. Hacker, J.J. Mc Cormack, J. Med. Chem. 29 (1986) 1370.
[53] G. Kotovych, J.W. Lown, J.P.K. Tong, J. Biomol. Struct. Dyn. 4 (1986) 111.
[54] J.W. Lown, C.C. Hanstock, R.D. Bradley, D.G. Scraba, Mol. Pharmacol. 25 (1984) 178.
[55] J.W. Lown, C.C. Hanstock, J. Biomol. Struct. Dyn. 2 (1985) 1097.
[56] D.A. Collier, S. Neidle, J. Med. Chem. 31 (1988) 847.
[57] S. Neidle, Chem. Br. 36 (2000) 27.
[58] D. Cairns, E. Michalitsi, T. Jenkins, S. Mackay, Bioorg. Med. Chem. 10 (2002) 803.
[59] K.X. Chen, N. Gresh, B. Pullman, Nucleic Acids Res. 14 (1986) 3799.
[60] H.D. Becker, J.Q. Chambers, in: Patiai (Ed.), The Chemistry of Quinonoid Compounds, Wiley, N. Y., 1974.
[61] H. Hartman, E. Lorentz, Naturaforsch Z. 7a (1952) 360.
[62] S.N. Singh, R.S. Singh, Ind. J. Pure Appl. Phys. 5 (1967) 342.
[63] J.D. McGhee, P.H. von Hippel, J. Mol. Biol. 86 (1974) 469–489.
[64] S. Nafisi, M. Hashemi, M. Rajabi, H.A. Tajmir-Riahi, DNA Cell Biol. 27 (8) (2008) 433–442.
[65] C.D. Kanakis, S. Nafisi, M. Rajabi, A. Shadaloi, P.A. Tarantilis, M.G. Polissiou, J. Bariyanga, H.A. Tajmir-Riahi, J. Spectrosc. 23 (1) (2009) 29–43.

Please cite this article in press as: J.S. Al-Otaibi, T.M. EL Gogary, Synthesis of novel anthraquinones: Molecular structure, molecular chemical reactivity descriptors and interactions with DNA as antibiotic and anti-cancer drugs, Journal of Molecular Structure (2016), http://dx.doi.org/10.1016/j.molstruc.2016.10.098